

# Modelling and instrumentation of a geotextile in the geotechnical centrifuge

S.Springman, M. Bolton, J. Sharma & S. Balachandran  
Cambridge University, UK

**ABSTRACT:** Scaling relationships in the geotechnical centrifuge have been considered for woven and grid soil reinforcements, and the stress-strain response of small scale models have been investigated. Instrumentation has been devised to measure load and strain independently.

## 1 INTRODUCTION

Understanding the behaviour of reinforced earth structures, particularly embankments and walls, has advanced significantly in recent years. Design theories have been developed alongside an increasing database of full scale (Fannin and Hermann 1990), small scale (Juran and Christopher 1989; Jewell et al 1992) and centrifuge model tests (Bolton and Pang 1982; Mitchell et al 1988; Jaber and Mitchell 1990).

However, few case studies have been instrumented to give data of soil-reinforcement load transfer (Yako and Christopher 1987). Most report load conditions at failure, external measurements of displacements and secondary estimations of soil or reinforcement strain (Liu et al 1991). These instrumented structures have used almost inextensible steel or aluminium reinforcements, for which the stress-strain modelling and gauge installation are relatively simple.

For more extensible geotextiles and geogrids, the effects of locked-in strains following compaction of fill, and the visco-elastic nature of polymeric materials, make it desirable to measure the tensile loads/unit width,  $T$ , and strains,  $\epsilon$ , independently (McGown et al 1990). Usually difficult to achieve in practice, such measurements obviate the need for a repeatable stress-strain calibration of these materials.

Quantifying this tension-extension distribution along any reinforcing elements is essential (Bolton 1990) if the progressive failure mechanisms are to be investigated. Bolton and Pang (1982) attributed the plastic stress redistribution, which occurred in centrifuge models of walls (reinforced by metallic strips or rods) during increasing acceleration, to successive rupture of reinforcing element layers followed by progressive take up of load in those

adjacent. In contrast, for similar centrifuge models, Jaber and Mitchell (1990) considered that the sudden shedding of reinforcement loads was due to stress redistribution in the sand and not strip rupture.

Current methods of analysis do not lead to successful displacement predictions for reinforced structures under working loads. This is particularly important for serviceability considerations when extensible geotextiles and geogrids are used. Prediction will be based on reinforcement stress-strain data obtained from element tests.

Clearly, the stress-strain response can be noticeably different for extension tests conducted 'in air' and 'in soil', however, the operational boundary conditions must also be replicated in these laboratory calibrations (Bolton 1990; Wu et al 1992). This paper outlines some of the properties of materials and their instrumentation from preliminary 'in air' extension tests, in preparation for a series of centrifuge model tests on reinforced embankments and walls.

## 2 MODELLING

A geometric characterisation of textile or grid reinforcement is shown in Figure 2.1a; width of longitudinal tensile strand  $b_1$ , lateral spacing between strands  $s_1$  gives a lateral aperture  $a_1 = s_1 - b_1$  (to form an open net if  $a_1 > 0$ ), and the similar width  $b_2$ , and spacing,  $s_2$  give aperture  $a_2$  created by lateral strands. For simplicity, all strands are taken to be of circular section. The tensile capacity will be proportional to the cross-sectional area of reinforcement/unit width of sheet,  $A (= \pi b_1^2/4s_1)$ .

The main integrated property of interest is the

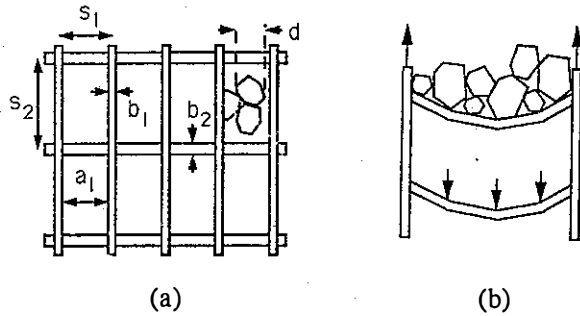


Fig. 2.1 Geometric characterisation of reinforcement

tensile capacity of area  $A$  measured at a given strain  $\epsilon$ , strain rate  $\dot{\epsilon}$  and temperature. The frictional bond between fibres must be correct if the tensile strength and stiffness of the textile they comprise is to be measured accurately; especially for non-woven varieties. Tensile test pieces of such reinforcement must therefore be confined at the appropriate lateral effective stress, but in the absence of any restraint caused by that confinement, McGown et al (1982).

An *ideal* model, centrifuged at earth's gravity times  $n$ , would comprise identical materials with all significant dimensions scaled down by factor  $n$ . Full-scale stresses and strains would then be duplicated. The soil would be scaled down in grading by factor  $n$ , containing reinforcement in which internal dimensions ( $b$ ,  $s$  etc.) were also scaled down by  $n$ , as would the spacing between layers or strips. Accordingly, the area  $A$  would be reduced by factor  $n$ , so that the strength  $T$  mobilized /unit width at any given strain would likewise be reduced by factor  $n$ . This is the first scaling requirement: it happens, however, that it is generally inconvenient to achieve this by reducing both strand diameters and spacings. It will be desirable to explore the possibility of retaining full scale strand diameter  $b$ , but to *increase* the spacing  $s$ . In evaluating whether this simplified approach will be satisfactory, it is necessary to consider the other major integrated property, frictional bond.

The frictional bond will depend on whether the longitudinal strands will participate in a sheet-like displacement, or slip relative to soil (particle diameter  $d$ ) in the intervening apertures. The ratio  $s_2/d$  will be significant in considering the possibility of relative movement between the reinforcement and the soil within the apertures, since a shear band formed in soil requires a thickness of  $5d$  to form. A ratio  $s_2/d < 5$  should force the soil particles to be trapped in the aperture so that the mesh acts as a perfectly rough sheet, at least until the lateral strands slip (woven), or break (grid). Even where  $s_2/d \gg 5$ , a grid will still act like a sand-encrusted sheet if the

pull-through resistance of strong lateral ribs exceeds the sliding resistance of both surfaces of the grid, which may give a criterion such as  $s_2/b_2 < 10$ .

If the longitudinal strands act individually, the bond area will apparently be reduced by a multiplication factor,  $f_a = (\pi b_1)/(2s_1)$ . The friction coefficient will be reduced by a further factor  $f_\mu$  from that for soil-soil to that for polymer-soil, although the resistance will also depend on a factor  $f_s$  relating mean contact stress around the strands to the effective overburden pressure. However, the dilation of the soil around individual strands could exceed any tendency for Poisson's ratio area reduction of the strand due to extension. The net cylindrical expansion would tend to arch stress away from the aperture onto the strands, so that the frictional bond of the net would approach that of the polymer sheet, with  $f_a f_s \rightarrow 1$ , irrespective of the behaviour of lateral strands or ribs.

Sheet action can also be promoted by the ability of the lateral strands (Figure 2.1b) to pick up forces from soil particles and transmit them by funicular action to the neighbouring longitudinal strands. For geogrids, we must consider not the funicular action of the ribs, but their capacity to distribute loads by beam action. The development of bond in nets and grids is clearly a complex phenomenon.

Pull-out tests have been used to determine bond capacity, but their analysis is notoriously difficult (Palmeira and Milligan 1990). Centrifuge model tests may be used to validate a strategy for obtaining frictional bond for different circumstances (various values of  $s/b$ ,  $s/d$  etc). When stable interlocking of soil is observed to occur in the apertures, a direct shear test can be specified to find the interfacial angle of shearing resistance of a grid or net. If the material is wrapped around a block in one half of a shear box, the soil in the other half may be forced to slide past it. If the lateral strands are weak, and rupture during the model test, this would indicate that friction could be developed reliably only on longitudinal strands. Shear tests on artificial sheets made of contiguous longitudinal strands could then be used. Finally, back-analysis of centrifuge model data may be used to ascertain the degree of arching onto the strands.

Of course, no model can be a precise analogue of any particular structure in the field. It will be necessary to quote significant prototype dimensions, groups and properties, by multiplying up model parameters, and separately consider whether these are broadly representative of real structures. It will have become clear that the significant prototype properties are: for tension,  $nT$  as a function of  $\epsilon$  under specified test conditions; for frictional bond  $f_a$ .

### 3 REINFORCING ELEMENTS

Table 1 shows manufacturing details and stress-strain response for a typical proprietary full scale multifilament woven geotextile and a monofilament geogrid. Similar data is given for semi-equivalent scaled model reinforcements (Figure 3.1; Table 2).

We may select a microtextile or grid for which the median centrifuge model soil particle diameter  $d_{50}$  may be adapted to give either the soil-sheet ( $s_2/d < 5$ ) or the soil-grid ( $s_2/d \gg 5$ ) shear behaviour (Table 2). In the latter case, where  $s_2/b_2 < 10$ , then a sheet model might also apply. For Microweave, however, the lateral strands rely simply on friction against the longitudinal strands, so they will probably be unable to contribute to bond in any way.

Extension tests were conducted to failure to evaluate the strength and stiffness of uninstrumented model reinforcement 'in air' using an Instron device. The influence of the restraining method on each 200 mm square geotextile test piece was investigated using either a simple clamping system or a windlass-roller device to reduce tensile stress at the clamp. However, the ultimate tensile strength  $T_{ult}$  was similar, and failure seemed to propagate from the grip region in both cases. ( $\epsilon$  was not accurately measured for the roller method.)

In comparison, Netlon's BS6906 test on 'Microgrid F' (20 °C), for a faster  $\dot{\epsilon} = 10$  %/min, gave  $T_{ult} = 9$  kN/m (c.f. 9 kN/m) at  $\epsilon_{ult} = 24\%$  (c.f. 17 %). Load at  $\epsilon = 1$  % was  $T_1 = 0.72$  kN/m. Similar tests by AKZO ( $\dot{\epsilon}$  unknown) on Microweave gave  $T_{ult} = 24$  kN/m (c.f. 18 kN/m),  $\epsilon_{ult} = 20$  % (c.f. 16%), with  $T \cong 18$  kN/m at  $\epsilon = 16$  % and  $T_1 \cong 2.38$  kN/m (c.f. 2.63 kN/m). This confirmed that the clamp restraining apparatus was effective, and this was used for subsequent load controlled tests up to 20% ultimate load on instrumented Microweave.

If the centrifuge tests impose  $n = 40g$  on the model, then the stiffness and scaled strength at  $\epsilon = 1\%$ , and strength at ultimate load are  $E_1$ ,  $nT_1$  and  $nT_{ult}$  (Table 2). It can be seen from Table 1 that the range of values produced by the full scale geotextiles are well bracketed by the range of model geotextiles.

In this paper, we will concentrate specifically on the calibration of the instrumented woven polyester multifilament geotextile. Ultimate load tests on 62 warp threads, from a 200 mm wide sample, gave a mean at failure of  $58 \pm 7.5$  N ( $\therefore T_{ult} = 18$  kN/m) at  $\epsilon = 18.2 \pm 1.4$  %, and compares well with the data in Table 2. This variation in failure load underlines

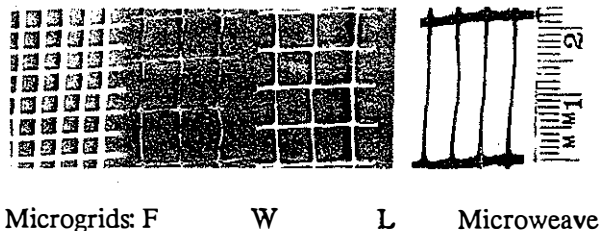


Fig. 3.1 Model reinforcements

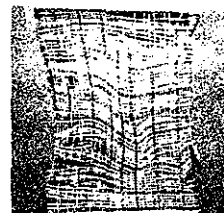


Fig. 3.2 Microweave: Progressive failure evidence

why progressive failure was observed for the geotextile test pieces (Figure 3.2).

### 4 INSTRUMENTATION

Evaluation of global displacements and local stress and strain may be achieved in several ways in prototype field tests, but with more difficulty at model scale. To obtain a sample of data at sufficient discrete points to evaluate the complex behaviour of a prototype, many miniature instrumentation devices must be installed. This will affect the local stress-strain fields by inducing a disturbance in the zone around the soil-geotextile that is to be monitored. Optimising these two effects is necessary, so that the instrumentation reveals, but does not change significantly, the soil-structure interaction mechanisms.

A method of instrumenting woven geotextiles with strain gauges for the measurement of tensile load has been developed at Cambridge (Sharma 1991). It has proved difficult to obtain repeatable calibrations of load and strain by fixing each end of the gauge directly to a single transverse (weft) strand of the multifilament, so an epoxy resin was used to create a stiffer, full-width (nominally plane strain) load cell section  $\cong 0.7$  mm thick, 5 grid apertures wide, on which the strain gauges were mounted (Figure 4.1).

Insulated copper wire strands, 0.4 mm diameter, were woven between the longitudinal (warp) filaments to provide a key to the epoxy, which was squeezed in a thin thread from a glue gun along the entire width. This section was sandwiched between

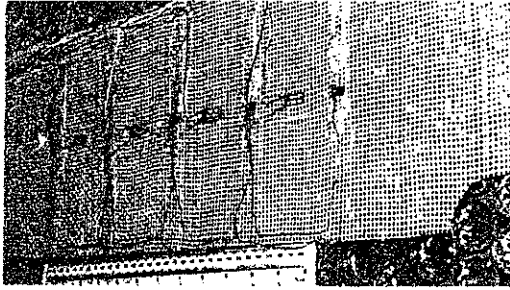


Fig. 4.1 Instrumented Microweave: Centrifuge test

two layers of cling film, and then clamped between a pair of parallel glass plates while the epoxy cured at room temperature. Great care was necessary to obtain a uniform hardened deposit of epoxy.

350  $\Omega$  self-temperature compensated constantan strain gauges, of 3.18 mm square active area on a 6.35 mm long polyimide strip, were glued centrally to the upper and lower surfaces of the epoxy strips using a cyanoacrylate adhesive, and wired into 2 arms of a Wheatstone bridge circuit. The two dummy gauges were 0-500  $\Omega$  variable resistors, which were located in the electrical junction box, close to the instrumented section. (Errors due to thermal effects may be reduced by keeping the gauges/resistors at the same temperature.) The bridge was wired to give tensile loading data and to eliminate bending effects. Offset voltages measured at zero load were removed by adjusting the resistors.

Post yield ( $10 < \epsilon > 20\%$ ) TML YL10 120  $\Omega$  Cu-Ni strain gauges, 10 by 3 mm active area on a 20 by 7 mm cellulose base (with 0-200  $\Omega$  dummy gauges) were attached to low stiffness backing strips created at other locations of the geotextile in an attempt to measure the longitudinal  $\epsilon$  in the fabric (Figure 4.1).

## 5 CALIBRATION

A 1 %/min strain control test (Table 2) was carried out on the virgin woven geotextile up to 50 % ultimate tensile strength (U.T.S.) in an Instron tensile tester. The results were evaluated to allow gauge calibrations of load/extension. In Figure 5.1, the slope to  $\epsilon = 1\%$  was relatively steep  $\approx 275$  kN/m, probably due to pre-strain induced during manufacture, which reduced by a factor of  $\approx 5$  for the next phase. The strain was held constant for some time periods, during which the material relaxed, with a resulting drop off in load. Upon reload, the initial response was stiff until the original curve was approached and rejoined, exhibiting typical elasto-

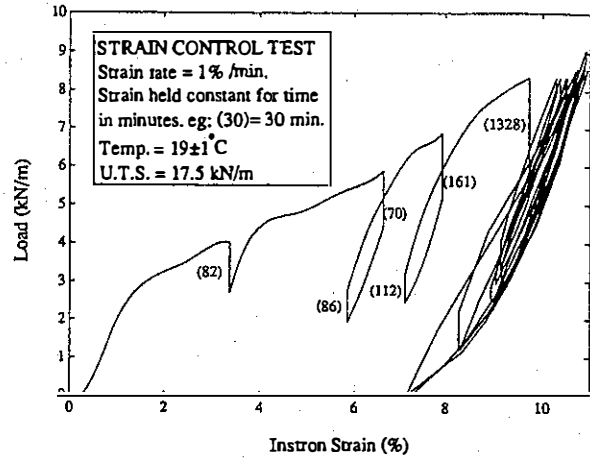


Fig. 5.1 Microweave tension test

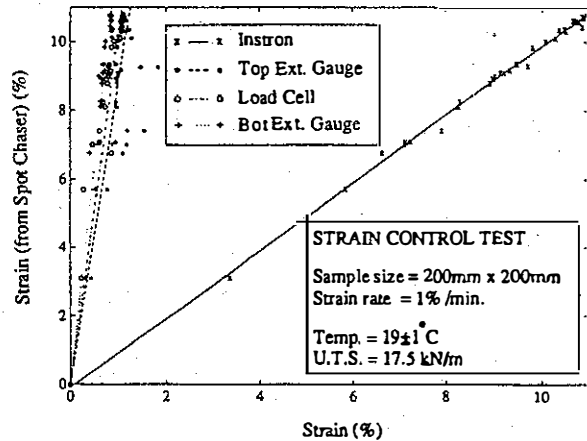


Fig. 5.2 Microweave: Comparison of strain

plastic behaviour combined with creep effects.

A series of 6 unload-reload cycles were carried out with brief pauses of  $< 7$  minutes at each extreme. Creep was observed, and the strain exhibited by the test piece increased at the same load, 8.3 kN/m. The cycles showed some hysteresis; greater with larger amplitudes. This was further followed by a set of 7 continuous unload-reload loops of varying amplitudes. It can be seen that nearly the same unloading curve was followed in all cases, and that on reloading the material took up the same load (8.5 kN/m) at an equivalent value of strain (10.8%). This augurs well for the repeatable calibration of the geotextile.

However, it must be noted that there was  $> 7\%$  permanent set and  $\approx 3.5\%$  elastic strain, following loading to 9 kN/m, 50% U.T.S. Since the model geotextile will need to be calibrated prior to the centrifuge test, a stress history record will be vital in subsequent interpretations of the strain. This will also

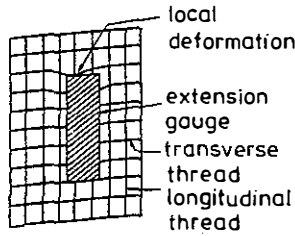


Fig. 5.3 Local restraint around an extension gauge

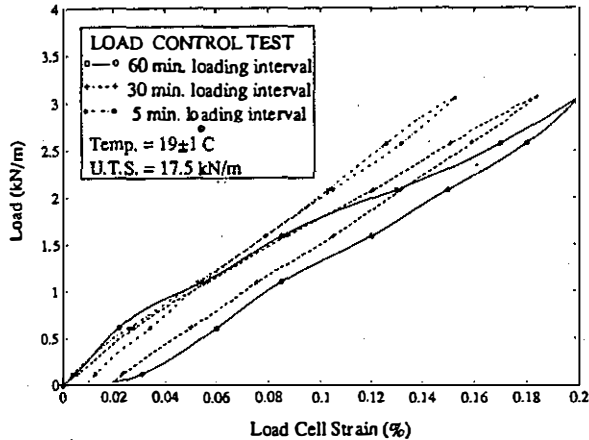


Fig. 5.4 Microweave: Time effect on load cell strain

have implications in modelling the unstretched and serviceability state of geotextiles in real life.

The values of 'Instron strain' were also compared against interpretations made from photographs taken at various stages during the test, using the Cambridge 'Spot Chasing' system (Phillips 1991). The results agreed within 2%. The actual strain experienced by each gauge was also calculated from voltage output and gauge factor and found (Figure 5.2) to be between 7-13% of the true strain. This local stiffening effect was expected for the load cell section, but the fixings of the extension gauges were intended to reduce this. The local deformation around a gauge (Figure 5.3) shows the restraint imposed on the woven threads in the warp direction.

Load controlled calibrations were also conducted up to 20% U.T.S. on the instrumented test piece (initially 200 mm square) to investigate the influence of time on the gauge readings. Increments of 0.5 kN/m were added to a hanger connected to the lower clamp, and left for periods of 5, 30 or 60 minutes. As expected (Figure 5.4), there was a significant time effect for the longer incremental loadings, in which hysteresis and non-linearity were marked. However, the actual gauge stiffness,  $E_1 \approx 38000$  kPa over the 5 minute loading period c.f. true strain values

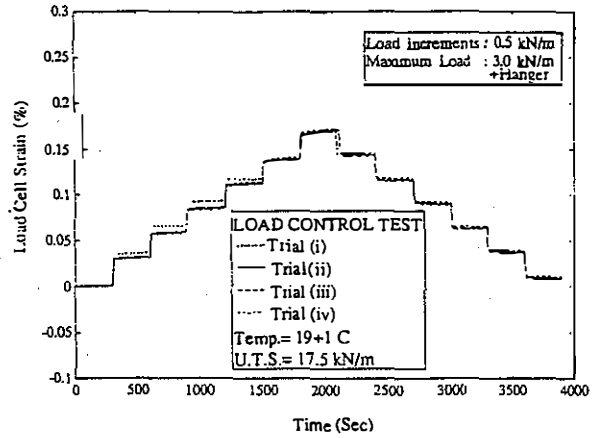


Fig. 5.5 Microweave: Load cell calibration

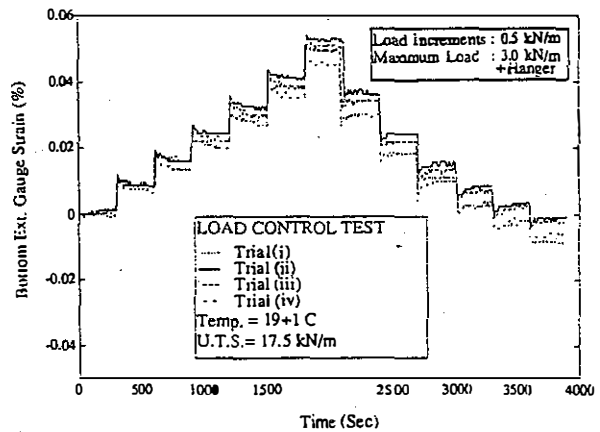


Fig. 5.6 Microweave: Extension gauge calibration

measured. 3 such load controlled tests (Trials ii-iv: Figure 5.5) gave repeatable indications of actual strain following the initial visco-elastic response from the first calibration (Trial i). This was not as repeatable for either of the two extension gauges, e.g. Figure 5.6 for the top cell, although it should be noted that their response was considerably stiffer, with a strain scale which is 5 times more sensitive.

## 6 CONCLUSIONS

Consideration has been given to the modelling of soil reinforcement behaviour in a geotechnical centrifuge. In-air T- $\epsilon$  data has been obtained using a new method of strain gauging woven geotextiles, and compared to known  $\epsilon$  from the Instron and photographic measurements. Repeatability was acceptable for load periods of < 5 minutes, as planned for centrifuge model tests on reinforced retaining walls constructed in sands. The extension strain gauges were not as effective.

## ACKNOWLEDGEMENTS

The cooperation of Mr Troost from AKZO and Dr Bush from Netlon is recorded with much gratitude. The contributions and skills of Messrs S. Chandler & T. Ablett (CUED) were invaluable.

## REFERENCES

- Andrawes, K.Z., K.H. Loke & K.C. Yeo. 1990. Application of boundary yielding concept to full scale reinforced and unreinforced soil walls. BGS ICRSS pp. 79-84.
- Bolton, M.D. & H.K. Pang. 1982. Collapse limit states of reinforced earth retaining walls. Geotechnique. Vol. 32, No. 4: 349-367.
- Bolton, M.D. 1990. Reinforced soil: laboratory testing and modelling. BGS ICRSS pp. 287-298.
- Fannin, R.J. & S. Hermann. 1990. Performance data for a sloped reinforced soil wall. CGJ 27:676-686.
- Jaber, M. & J.K. Mitchell. 1990. Behaviour of reinforced soil walls at limit state. BGS ICRSS.
- Jewell, R.A. et al 1992. to be published, Wroth Memorial Symposium. Oxford.
- Juran, I. & B. Christopher. 1989. Laboratory model study on geosynthetic reinforced soil retaining walls. ASCE. JGED Vol. 117, No. 7:905-925.
- Liu, L-Y., M-R. Wang & E-D. Ding. 1991. Centrifugal tests of mechanism of geotextile-reinforced soft foundation under breakwater. Centrifuge 1991. pp. 319-324. Rotterdam, Balkema.
- McGown, A., K.Z. Andrawes & M.H. Kabir. 1982. Load extension tests on geotextiles confined in soil. Proc. 2nd IC Geo. Las Vegas. Vol 3:793-798.
- McGown, A., K.C. Yeo & I. Yegarajah. 1990. Identification of a dynamic interlock mechanism. BGS ICRSS pp. 377-380.
- Mitchell, J.K., M. Jaber, C.K. Shen, Z.K. Hua. 1988. Behavior of reinforced soil walls in centrifuge model tests. Cfuge 1988. pp. 259-272. Balkema.
- Palmeira, E.M. & G.W.E. Milligan. 1990. Large scale pull-out tests on geotextiles and geogrids. GG&RP Balkema, Rotterdam. pp. 743-746.
- Phillips, R. 1991. Film measurement machine. User Manual. CUED/D-Soils/TR246.
- Sharma, J. 1991. Centrifuge modelling of reinforced embankments on soft soils. CUED Report :TRRL.
- Wu, J. & F. Tatsuoka. 1992. Discussion: Laboratory model study on geosynthetic reinforced soil retaining walls. ASCE JGE Vol. 118, No. 3: 496-501.
- Yako, M.A. & B.R. Christopher. 1987. Polymerically reinforced retaining walls and slopes in North America. NATO ARW APRSRS pp. 239-283. Ontario. Kluwer Academic Publishers.

Table 1. Manufacture details and stress-strain characteristics of full scale geotextiles

Geotextile & manufacturer	Type of geotextile (warp / weft)	A/m width mm <sup>2</sup>	b <sub>1</sub> mm	s <sub>1</sub> & s <sub>2</sub> warp/weft mm	ε %/min (@ °C)	T <sub>1</sub> (ε=1%) kN/m	E <sub>1</sub> = T <sub>1</sub> /A kPa	T <sub>ult</sub> kN/m	ε <sub>ult</sub> %	Failure type
Stabilenka 400 (AKZO)*	Woven polyester / polyamide	395	0.7	≡ Sheet (0.73)	1 20+/-2	25	63290	400	10	progressive
Tensar SR80 (Netlon)**	Polyethylene / polyethylene	404	6.4#	150 / 16	2 20+/-2	6.6	16337	71	14	progressive

\*Sample: 500 mm long. \*\*Sample: 336 x 336 mm square: 95% lower confidence limit. # Ribs: 1.4 mm thick, minimum width 6.4 mm

Table 2. Stress-strain characteristics of model geotextiles

Geotextile prototype & model	A / m width mm <sup>2</sup>	b <sub>1</sub> & b <sub>2</sub> mm	s <sub>1</sub> & s <sub>2</sub> mm	d <sub>50</sub> mm	s <sub>2</sub> / d	s <sub>2</sub> / b <sub>2</sub>	f <sub>a</sub>	T <sub>1</sub> kN /m	E <sub>1</sub> kPa C	T <sub>ult</sub> kN/m C R	ε <sub>ult</sub> % C	Failure type	nT <sub>1</sub> kN /m	nT <sub>ult</sub> kN /m
Polyester Microweave	53	0.7*	3.3 & 3.4	0.12 & 0.9	28 & 4	5	0.21	2.6	49057	18 17 18	16	progressive	105	720
Polypropylene Microgrid F	28.5	0.4#	4.4 & 21.4	0.9 & 1.7	24 & 12	14	0.14	1.1	38596	9 8 8	17	sudden	44	360
Polypropylene Microgrid W	22	0.4	5.7 & 6.3	0.22 & 1.7	28 & 4	16	0.11	0.43	19545	3 3 3	23	sudden	17	120
Polyethylene Microgrid L	5.7	0.2	5.5 & 7.1	0.22 & 1.7	32 & 4	36	0.06	0.15	26316	1 1 1	12	sudden	6	40

ε = 1 %/min, 19+/-1 °C. Samples: 200 x 200 mm. Restraint: C = clamp, R = roller. \* Flat not circular thread. # Rib minimum diameter. n = 40.